Bulletin of the Mineral Research and Exploration

http://bulletin.mta.gov.tr

Reservoir characteristics of the middle Eocene Avanah Formation in Erbil governorate, northern Iraq: integration of outcrop and subsurface data

Wrya J. MAMASENI[a], Irfan Sh. ASAAD[a,b*] and Ali I. AL-JUBOURY[c]

[a] *Salahaddin University-Erbil, College of Science, Department of Earth Sciences and Petroleum, Erbil, Iraq*
[b] *Knowledge University, College of Engineering, Department of Petroleum Engineering, Erbil, Iraq*
[c] *Al-Kitab University, College of Engineering, Petroleum Engineering Department, Kirkuk, Iraq*

Research Article

Keywords:
Avanah Formation, Erbil, Middle Eocene, Northern Iraq, Reservoir Properties.

ABSTRACT

The current work investigate the petrophysical characteristics of the Middle Eocene Avanah Formation in the Erbil Governorate using IP software to analyze the well data, integrated with the petrographic investigation of the formation in the nearest outcrop in the Gomaspan section. Well logging data revealed that the main lithology of the formation is limestone and dolostone while the lithology in the Gomaspan section is composed of limestone, dolomitic limestone, marly dolomitic limestone, and thin beds of shale. The lower dolomitic unit in the subsurface section of the formation is believed to be the most suitable reservoir unit due to good petrophysical characteristics including, low water saturation, high porous medium, and the presence of movable hydrocarbon. To measure porosities, a variety of well logging techniques were used in this study. The investigated formation was divided into Avanah dense (limestone unit) and Avanah porous (dolostone unit) based on their porous components. The petrographic study shows that most pore types of the formation are secondary and represented mainly by vuggy, moldic, intercrystalline, and fracture types. Most of the fractures in the upper limestone units are filled by calcite cement. The study claimed that the lower part of the formation (dolostone unit) in both sections is considered a good reservoir.

Received Date: 20.10.2023
Accepted Date: 15.03.2024

1. Introduction

The well logging technique is widely used in subsurface projects to provide petrophysical estimations and calculate the physical characteristics of the rocks as well as the liquid (gases, hydrocarbons, and water), (Catuneanu, 2006). Reservoir assessment involves finding, identifying, and extracting hydrocarbons from a reservoir. These methods might be used at every stage of the hydrocarbon exploration and production process (Gonfalini, 2005). Petrophysical examinations of the reservoirs, mineralogical identification, and well log links must be carried out in order to generate a valid overall performance estimate (Tiab and Donaldson, 2004). Carbonate rocks have significant concern in reservoir studies because most of the hydrocarbon reserves in the world are stored in their pore spaces and more than 50% of them are produced oil (Yang, 2017). The determination of the characteristics of the carbonate rocks through petrographic investigation is critical in controlling their pore system and aids in more comprehension of their reservoir properties (Asaad et al., 2022*a*; Balaky et al., 2023).

Few studies have been conducted on the reservoir characteristics of the Avanah Formation, Al-Hamdany and Sulaiman (2014) described the porosity of it in

Citation Info: Mamaseni, W. J., Asaad, I., Al-Juboury, A. I. 2024. Reservoir characteristics of the middle Eocene Avanah Formation in Erbil governorate, northern Iraq: integration of outcrop and subsurface data. Bulletin of the Mineral Research and Exploration 175, 1-17. http://doi.org/10.19111/bulletinofmre.1453586

**Corresponding author: Irfan Sh. ASAAD, irfan.asaad@su.edu.krd*

wells (K-149, K-319, and K-339) in Avanah dome and wells (K-432 and K-117) in Khurmala dome and concluded that the lower and middle units are porous dolomitic in spite to the upper part which is relatively dense limestone. Musheer (2021) evaluates the reservoir properties of the formation using Techlog software of Schlumberger for the drilled wells in the Khurmala dome and concluded that the gas zone of all wells is concentrated in the upper part of the formation and the oil zone is situated in the lower part. Asaad (2022) and Asaad et al. (2022*b*) have both studied the Avanah Formation in the Gomaspan section. The former study primarily examined the microfaceis and depositional environment, while the latter studied the petrography and mineralogy of the attractively rinded iron oxide-carbonate concretions in the lower part of the formation.The current study aims to identify the petrophysical and lithological parameters of the Avanah Formation to evaluate the reservoir characteristics based on the available well logs collected from the well XX0 in the Khurmala oilfield combined with the petrographic description from a surface section in the Gomaspan area.

2. Location of the study area

Two sections from the surface and subsurface were selected for this study. The subsurface section in the Khurmala oilfield, (Figure 1), is located in Erbil Governorate, 35 km southeast of Erbil city, between the Zurgazraw area and the Hawler plain (near Helawa Village). This oilfield is located within an intraplate basin in the Low Folded Zone on the Arabian platform's northeast border (Figure 1a). The studied area is a part of the Zagros Fold-Thrust Belt, which is made up of a series of widely spaced, gentle folds with a moderate amplitude (Fouad, 2012). The study area is structurally a part of the Kirkuk structure, an anticline running from northwest to southeast that is divided into three major structural domes by two noticeable saddles: The Dibagah saddle divides Avanah Dome from Khurmala Dome and the Amsha saddle divides Baba Dome from Avanah Dome (Figure 1c). Whereas the Gomaspan outcrop is situated approximatly 30 kms northeast of Erbil city on the Erbil-Dolly Smaquli main road, in the southwestern limb of Bna Bawi Anticline (Figure 1b) in the boundary between High Folded Zone and Low Folded Zone (Asaad et al., 2022*b*).

The formation in the investigated well is divided into two parts: the shallower unit, which is primarily limestone and has a thickness of approximately 90m, and the deeper unit, which is predominantly dolostone and has a thickness of about 120m. While in the Gomaspan outcrop section, it consists of 56m of medium to thick beds of grey dolomitic limestone, yellow limestone, and blue marly dolomitic limestone intercalated with thin beds of blue marl and dark grey shale and thin-to medium-bedded limestone intercalated with red mudstone in the upper part. The Formation belongs to the Middle-Upper Eocene cycle (Buday, 1980). The nature of its lower and upper contacts in the Khurmala oilfield is unconformable with both upper limestone beds of the Khurmala Formation and lower limestone with anhydrite beds of the Fatha Formation respectively. Whilst, in the Gomaspan section, occur as a tongue inside the clastic rocks of the Middle Eocene Gercus Formation (Asaad, 2022, Figure 1d).

3. Materials and methods

In this work, the log open-hole data from the examined well was analyzed along with deeper and low resistivity, neutron porosity (NPHI) and bulk density (RHOB) in addition to gamma rays (GR) data in a digitized LAS file with one reading every 0.15m depth. The gamma-ray was employed for correlation and differentiation of non reserve units. Neutron and density records were utilized to identify the major reservoir intervals. Avanah Formation was separated into two reservoir zones: the upper Avanah dense (AD) and lower Avanah porous (AP). The logging analysis was performed by the Interactive Petrophysics software (IP4.4), which included identifying fluid and wellbore properties based on the logging curve's subtitle in addition to designing the Buckles model to examine formation permeability using diagonal lines between porosity and water saturation.

The petrographic study of the carbonate beds of the Avanah Formation in the Gomaspan outcrop was obtained from 29 thin sections in order to investigating the petrographic components, diagenetic processes, and porosity types of the formation. The Alizarine

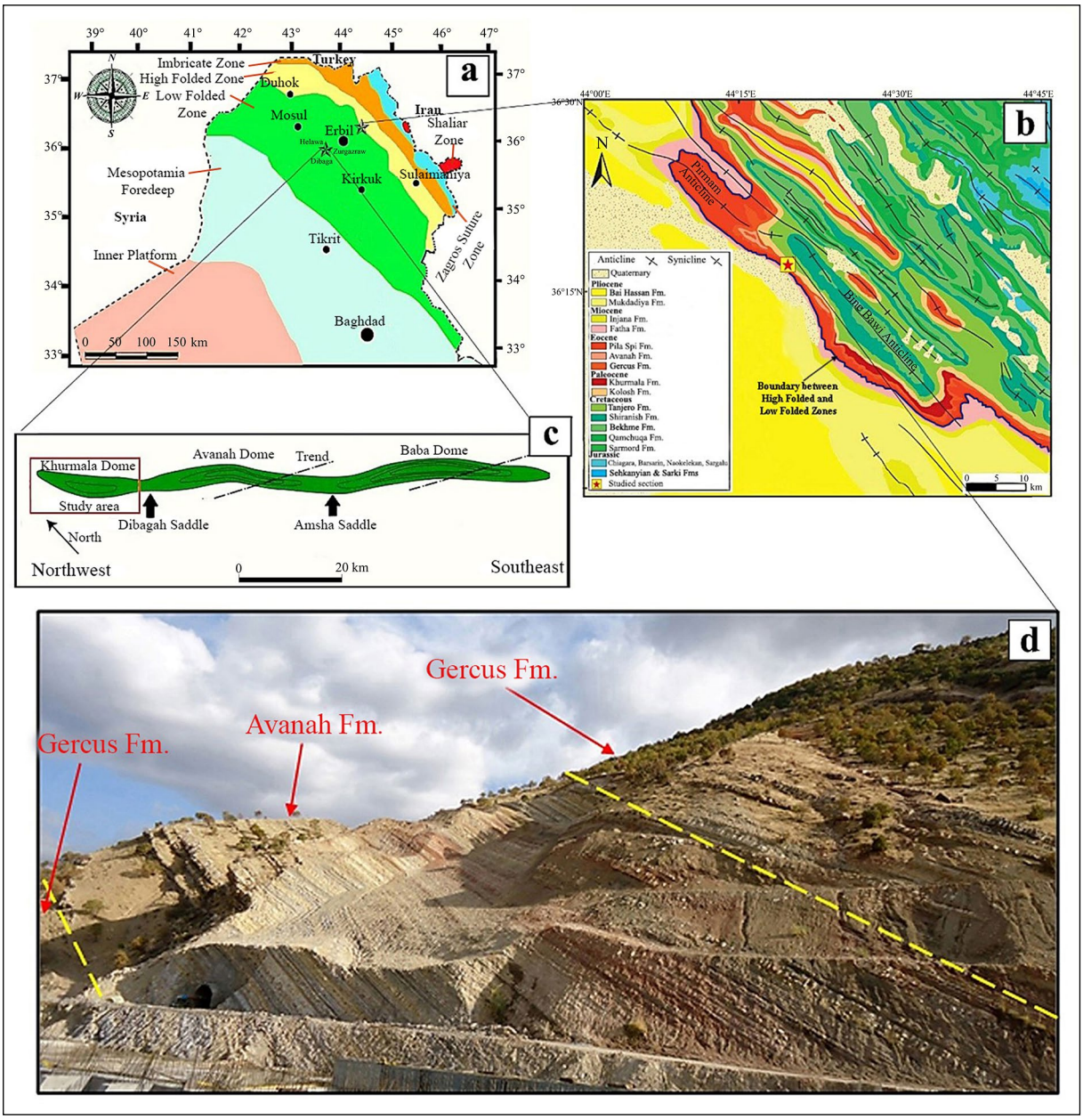

Figure 1- a) Location map of studied sections with tectonic subdivision of Iraq, b) Geologic map of Gomaspan area after (Awdal et al., 2013), c) Three domes of the Kirkuk oilfield included the studied dome, d) The succession of Avanah Formation in the Gomaspan outcrop lensed in red mudstone of Middle Eocene Gercus Formation.

Red Solution (ARS) was used for staining the thin sections following the Friedman (1959) procedure to discriminating between calcite and dolomite.

4. Results

4.1. Petrographic and Diagenetic Overview

The microscopic investigation of the limestone, marly limestone and dolomitic limesotone of Avanah Formation in the Gomaspan surface section showed that the micrite is the main groundmass that partly changed to microspar due to recrystallization. The main skeletal grains of the formation are benthonic foraminifera (Figures 2a and b), calcareous green algae (Figure 2b), ostracoda (Figure 2c), calcispheres (Figure 2c), pelecypods (Figure 2a) and bioclasts. Whereas, non-skeletal grains are peloids (Figure 2b), oncoids (Figure 2d), intraclasts (Figure 2b), and monocrystalline quartz (Figure 3a). Diagenetic

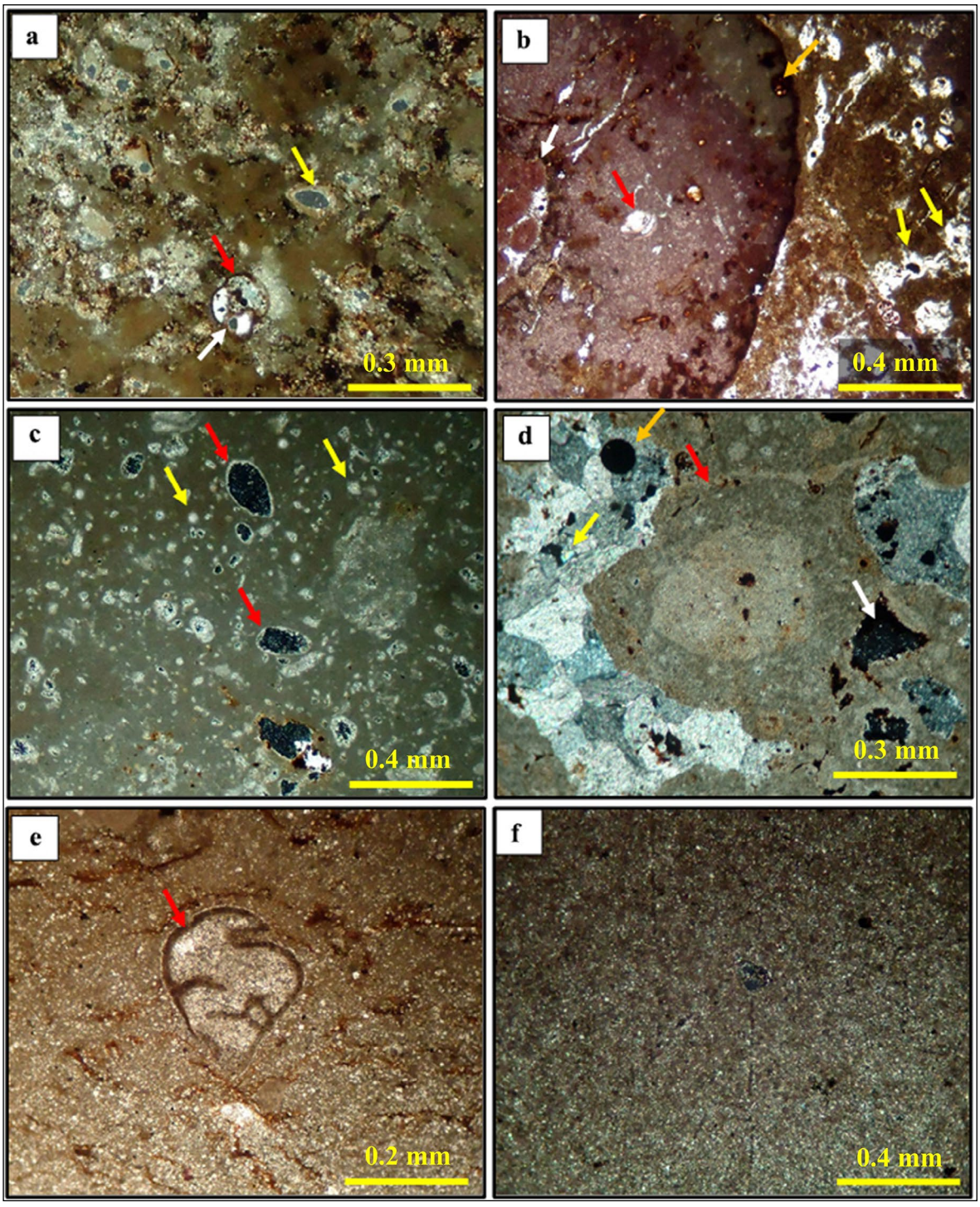

Figure 2- Photomicrographs of the Avanah carbonate in the Gomaspan outcrop showed: a) benthonic foraminifera (*Valvulina* sp.) (red arrow) affected partially by dissolution forming intraparticle porosity (white arrow) and pelecypods mold forming mold porosity (yellow arrow) within marly limestone beds. AG. 17., X.N. b) Benthonic foraminifera (rotaliids) (red arrow), in large intraclasts (orange arrow) and there is a packed peloids in its left side (white arrow), calcareous green algae (yellow arrows) within dolomtic limestone beds. AG.15., P.P. c) Molds of ostracoda (red arrows), calcispheres (yellow arrows) within dolomitic limestone beds. AG.9., X.N. d) Oncoids (red arrow). Spherical pyrite (orange arrow) and monocrystalline quartz (yellow arrow) within the fracture-filled blocky calcite cement. Vuggy pores formed a triangular shape partially filled by pyrite (white arrow) within marly dolomtic limestone beds. AG.2., X.N. e) Micrite envelopes developed around the benthonic foraminifera's test witihn dolomitic limestone beds. AG.15., P.P. f) Unimodal, very fine to fine-crystalline planar-s (subhedral) mosaic dolomite texture within dolomitic limestone beds. AG.21., X.N.Key:AG=Avanah-Gomaspan, P.P: Plane polarized light, X.N: Crossed Nicols.

processes affected the rocks of the formation started with micritization which was exhibit as rims and envelop around the skeletal grains (Figure 2e). Both early and late stage of dolomitization were observed in the carbonate rocks of the Avanah Formation. The early stage of it which is unimodal, very fine to fine- crystalline planar-s (subhedral) mosaic dolomite texture according to Sibley and Gregg (1987). It is characterized by scattered dolomite crystals that are less than 60 μm replacing subtidal carbonate muds in the lower and upper parts of the Avanah Formation (Figure 2f). Late stage dolomitization characterized by unimodal, fine to medium crystalline planar-s (subhedral) mosaic dolomite texture which is dominate in the lower part of the studied section and subjected to dissolution (Figure 3a). Cementation filled the fractures and pores of the Avanah carbonate and display by granular calcite cement (Figure 3b) which common in the lower part, blocky calcite cement (Figure 2d) and iron oxide cement (Figure 3c) that predominate in the upper part. Chemical compaction (stylolites) was noticed in the upper part of the Gomaspan which are sutured seam stylolite, irregular type with peaks of low amplitude (Wanless, 1979) and filled with iron oxide cement. Opaque pyrite crystals were observed in different parts of the Avanah Formation (Figure 2d). Selective silicification is occurred in the upper part of the formation affecting the skeletal grains associated with organic matters of the Avanah carbonates (Figure 3d).

4.2. Parameters of the petrophysical properties

Petrophysical properties of the Avanah Formation in Khurmala oilfield have been determined by using various parameters based on well log data, these include; shale volume, porosity(φ), water saturation (Sw), and the main lithological composition.

4.2.1. Shale Volume

The gamma-ray log is the principal reservoir tool for determining the amount of shale. Measurement of V_{shale} for young rocks is the initial stage. The following formula (Equation 1) can be used to compute the gamma-ray index (IGR):

$$IGR = \frac{GRlog - GRmin}{GRmax - GRmin} \quad (1)$$

Where: GRlog is the formation's gamma-ray reading, GRmin is the minimum gamma-ray reading (clean sand or carbonate), and GRmax is the greatest gamma-ray reading (shale).

In the petroleum sector, the common technique for determining shale volume for early rocks is given as Equation (2) (Asquith and Krygowski, 2004):

$$Vsh = 0.33(2^{2*GRI} - 1) \quad (2)$$

The maximum and minimum numbers of gamma ray are necessary to calculate the amount of shale in each formation depending on the lithological components of the formation. According to Figure 4, the Avanah limestone has a maximum gamma reading of 36 and a minimum gamma ratio of 0.8. The readings increase along the gamma curve to 5.2 and 62 at the dolomite-containing bottom portion. The dense section of the Avanah has an average clay content of 4%, while it about 8% in the porous part, indicating that the selected formation typically contains no more than 10% clay.

4.2.2. Pickett Cross-Plot Model

Pickett (1972) introduced a cross-plot, that is a graphical depiction of Archie's concept. The parallel lines which indicate the water saturation (Sw) maybe produced by charting the real resistivity (Rt) on the horizontal axis and the effective porosity (φe) on the vertical axis utilizing logarithmic scales for both axes. Any plotted point's Sw can be read in full. This method is predicated on the concept that cementation factor (m), water saturation, and porosity have an impact on actual resistivity. The wet resistivity (RO) is represented by the line at 100 percent water saturation. Water resistivity can be read on the actual resistivity scale where porosity equals one, and the line with a slope of (-1/m) intercepts the vertical scale. The link between effective porosity and real resistivity shows that the Avanah Dense (AD) has a water resistance of 0.014 (Figure 5) while the formation water resistivity in the other part (AP) is too low (0.003) and this relationship moreover been applied to calculate the values of a, n, and m parameters (Figure 6).

4.2.3. Bulk Volume Water (BVW) or Buckles Model

Calculating the bulk volume of water involves using a cross plot of porosity and water saturation.

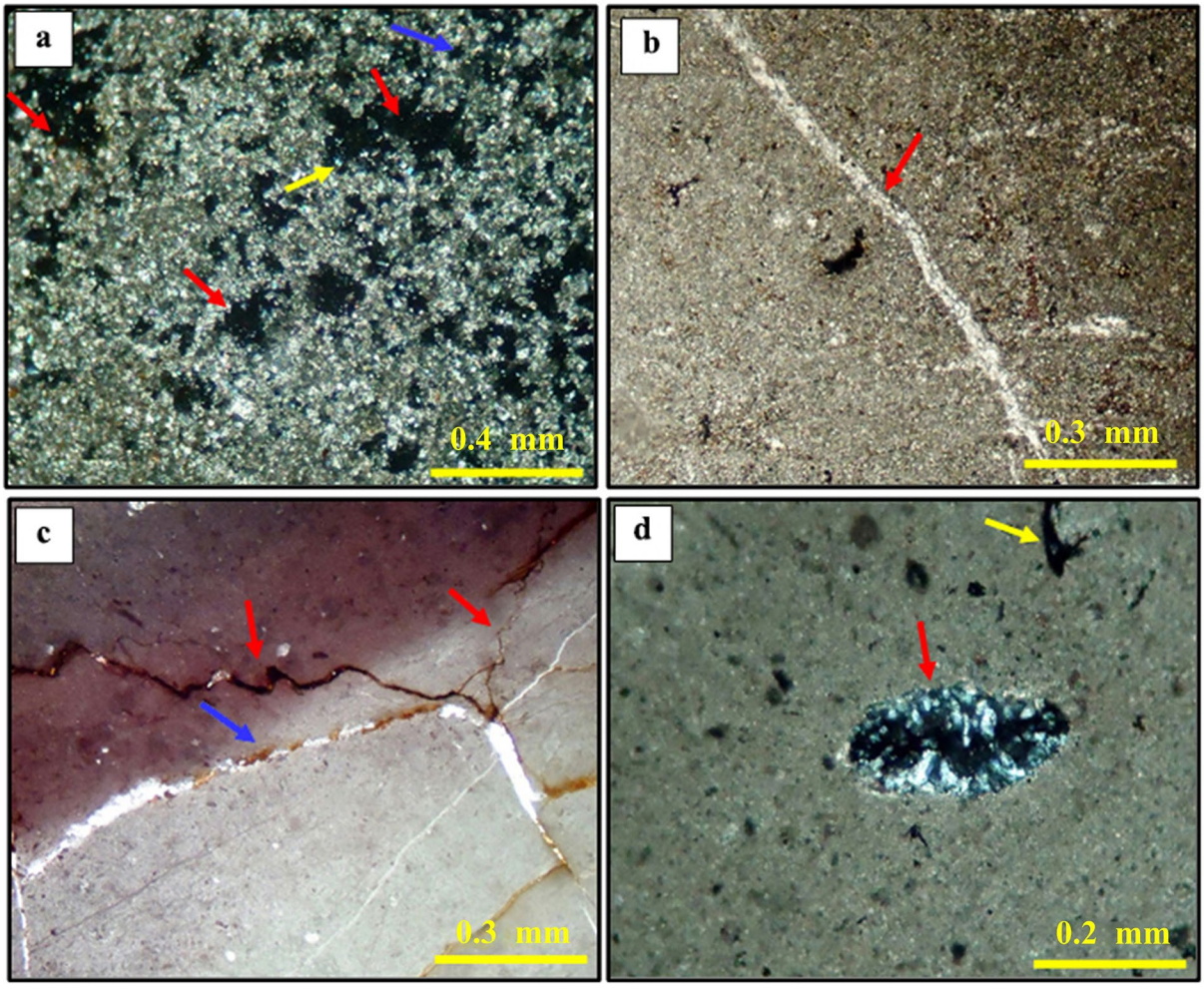

Figure 3- Photomicrographs of the Avanah carbonate in the Gomaspan outcrop displaying : a) Fine to medium crystalline planar-s (subhedral) mosaic dolomite texture subjected to dissolution forming vuggy porosity (red arrows) and intercrystalline porosity (blue arrow) and including monocrystalline quartz (yellow arrow) within dolomitic limestone beds.AG.4. X.N. b) Fractures filled with granular calcite cement (red arrow) within marly limestone beds. AG.25. P.P. c) Sutured seam stylolite, an irregular type with peaks of low amplitude filled by iron oxide cement(red arrows)and fractures partially filled by iron oxide cement (blue arrow) within limestone beds. AG.28. P.P. d) Selective silicification (chert) affected the ostracod's carapace (red arrow) surrounded by organic matter (yellow arrow) within dolomitic limestone beds. AG.24. X.N.

It is crucial to understand the total volume of water and the irreducible saturation of water (Swirr) because the amount of produced water in a well might have an impact on the well economy (Asquith and Krygowski, 2004). When the volume of bulk water follows hyperbolic lines and is constant or nearly constant, the composition is homogenous and at irreducible water saturation (Swirr).

In the present work, the dolomite part of the Avanah Formation is equally dispersed around the hyperbolic line 0.02 (Figure 7). This means that the reservoir is homogenous and irreducibly saturated with water. In contrast, the other part of the formation, which is composed of limestone, contains more water. As a result of the formation water concentration growing when the majority of the water from the hyperbolic lines is spread (the points have random distributions or not spread equally along the hyperbolic line).The data points may be dispersed, as seen in Figure 8 if there the rock type is porous, vuggy or fractured. This is the reason why in some reservoirs with complicated pore networks, this type of cross plot cannot be utilized to detect moving water.

Considering Figures 7 and 8, the data points on the bulk volume water cross plot of the dolomite in the

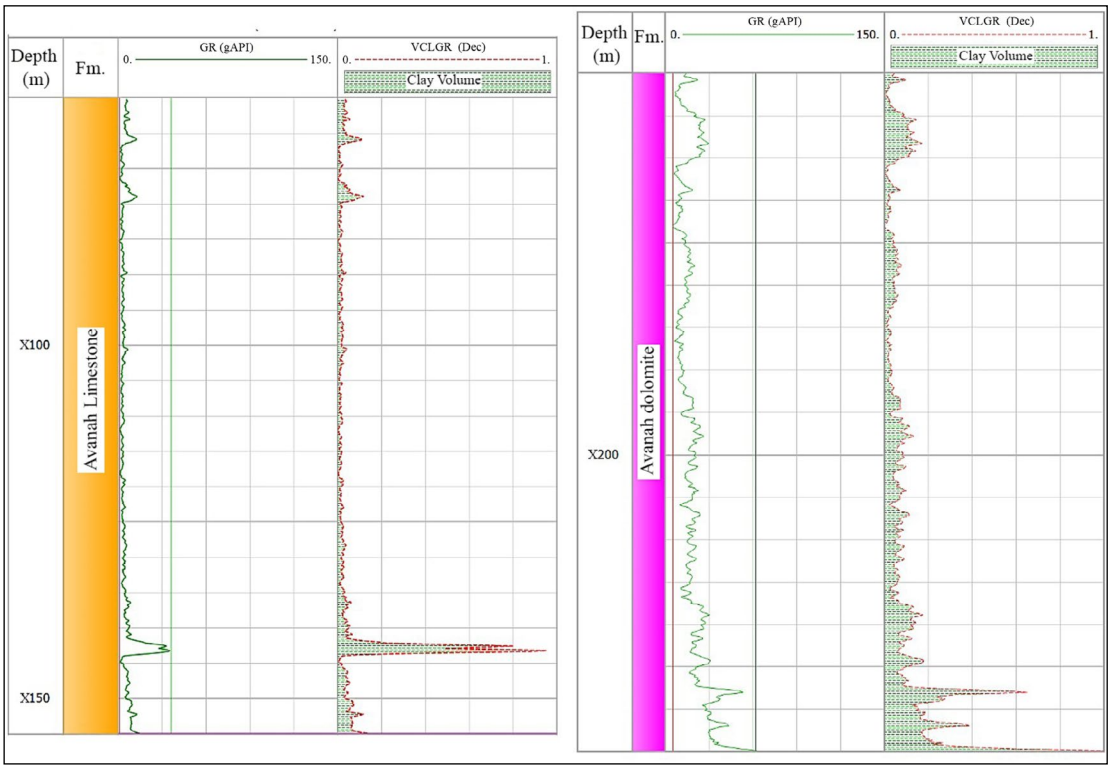

Figure 4- Clay volume within the both units of the studied Avanah Formation.

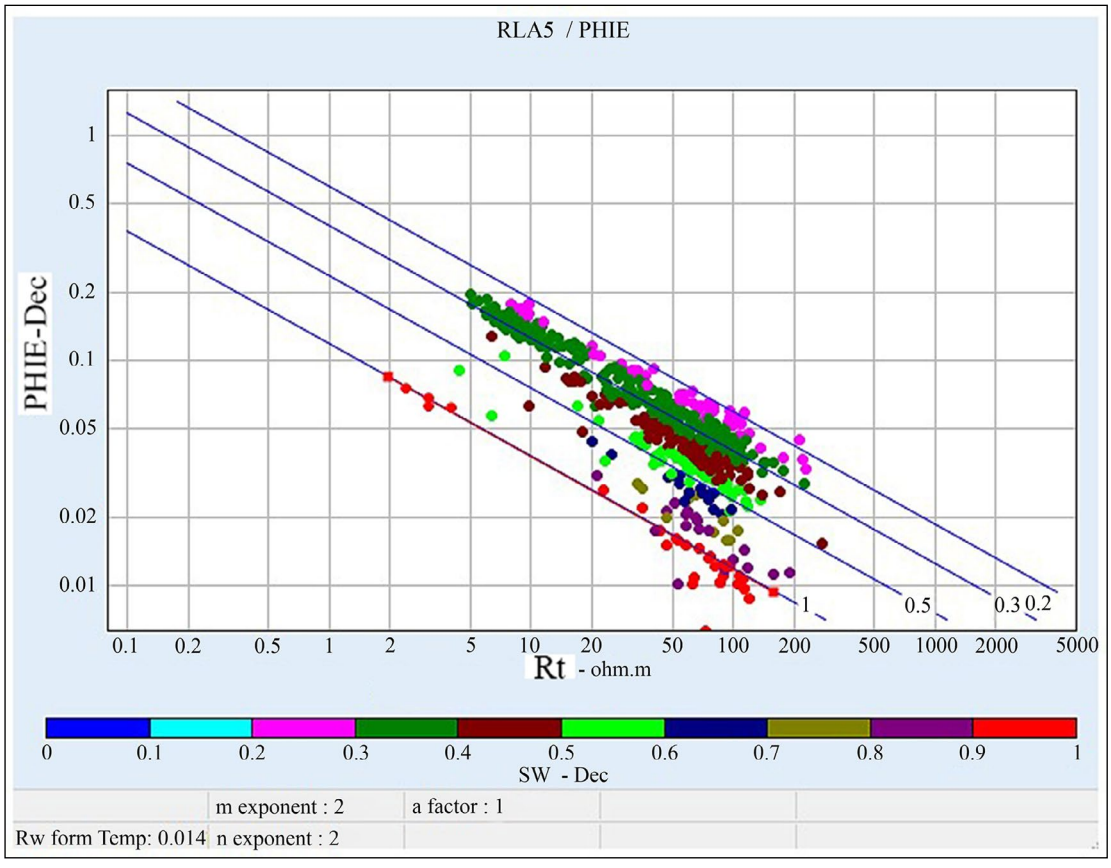

Figure 5- Effective porosity (PHIE) versus resistivity (ILD) plot (Pickett′s plot) for water saturation determination at AD zone.

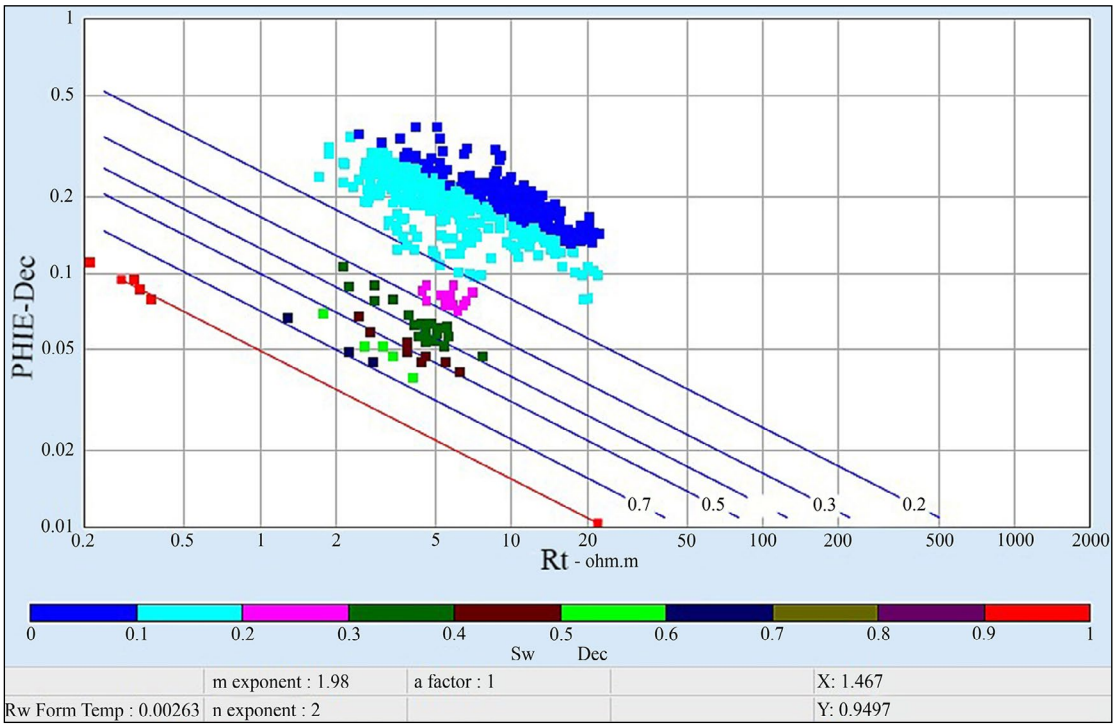

Figure 6- Effective porosity (PHIE) versus resistivity (ILD) plot (Pickett′s plot) for water saturation determination at AP zone.

Avanah Formation show the best clustering (data-point scatter from the hyperbolic line 0.02) or a coherent pattern to one of the curved hyperbolic lines, referring that the reservoirs are at irreducible water saturation and thus will not produce water. The reservoir would have a depressed water cut. There is no mobile water, which can be held by capillary pressure in these intervals since they are produced oil.

Water saturation levels and bulk volume water values are both low, having not exceeded 10 percent. As a result, the reservoirs wouldn't see any water cuts. On the other hand, the lack of clustering (data-point scatter from the hyperbolic line between 0.01-0.06) or incoherent pattern to one of the curved hyperbolic lines on the bulk volume water cross plot of the Avanah limestone indicates that the reservoirs are not exactly at the irreducible water saturation and will therefore produce some water relative to oil. Typically, these intervals are created relative to oil and include mobile water than can be held by capillary pressure. The bulk volume water values and the water saturation values are both high, reached to 35%. The reservoirs would therefore have a significant water cut.

4.2.4. Porosity Model

Porosity is defined as the volume of the liquid-filled non-solid portion of the rock divided by the total volume of the rock (Crain, 1986). The porosities determined from logs without accounting for the presence of clay are referred to as total porosities. Effective porosity, on the other hand, refers to the pore space where bound water and hydrocarbons are found (Nnaemeka, 2010), whereas resultant porosity is measured after clay's impact has been taken into consideration. If there is no shale, total porosity equals effective porosity. The relationship between total porosity (φt) and effective porosity (φe) is shown by the equations (3, 4). Carbonates typically include pore (secondary porosity) networks that are both very varied and complex. This implies that the conversion of porosity to permeability and multi-phase flow properties is quite challenging (Hamon, 2003; Gomes et al., 2008; Neilson and Oxtoby, 2008; Blunt et al., 2012). The porosity of modern carbonates ranges from 40 to 70%, while that of lithified older samples is just 5 to 15%, according to Choquette and Pray (1970). Carbonates lose some of their porosity primarily as a result of pressure dissolution, compaction, or cementation (Mukherjee and Kumar, 2018). Because

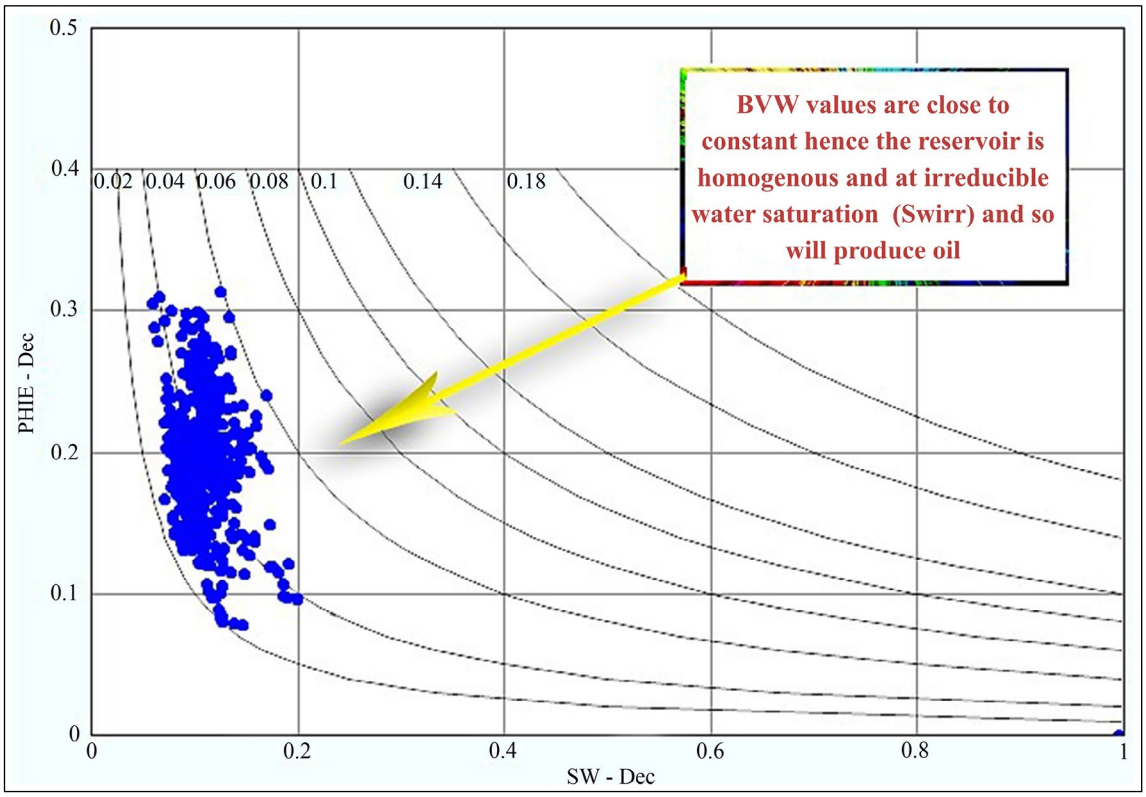

Figure 7- Porosity versus Water Saturation plot for well XX0 showing the constant or close hyperbolic pattern reffering that the reservoir is at irreducible water saturation.

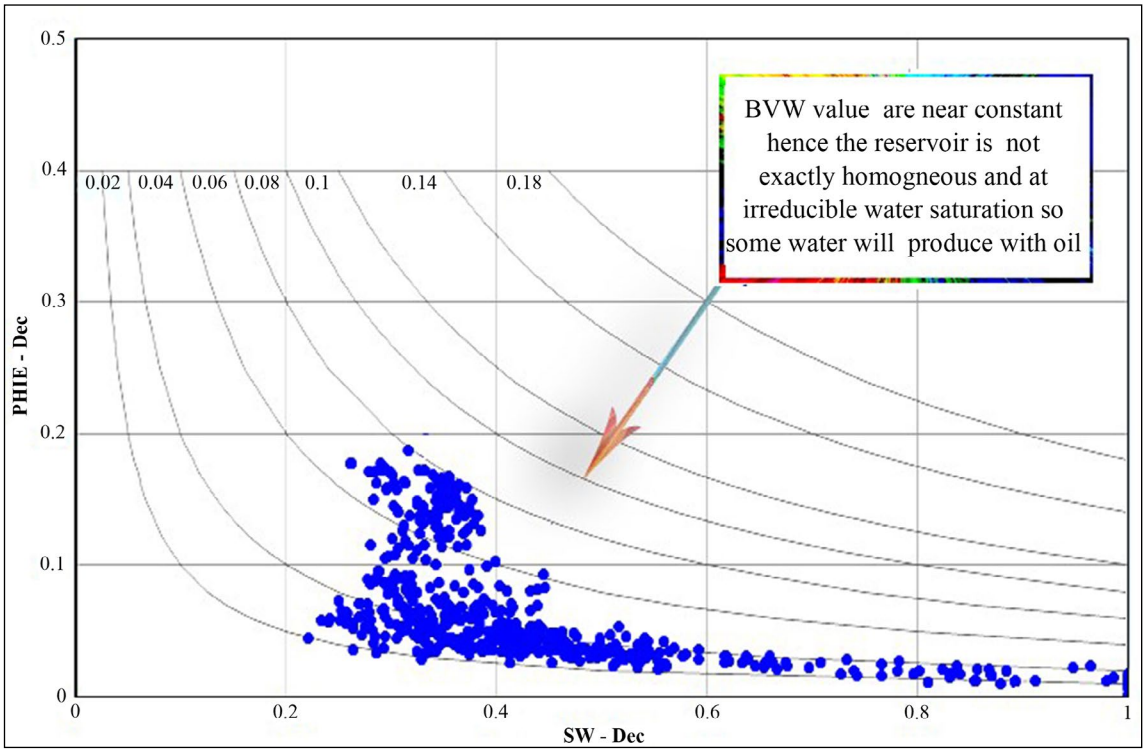

Figure 8- Porosity versus Water Saturation plot for well XX0 showing the constant or close hyperbolic pattern reffering that the reservoir is at irreducible water saturation.

the shale content of the Avanah Formation fluctuates between 4% and 8%, there is no discernible difference between effective and total porosity. Porosity values are calculated using adjusted density-neutron logs (Asquith and Krygowski, 2004).

$$\varphi t=(\varphi N+\varphi D)/2 \quad (3)$$

$$\varphi e=\varphi t*(1-Vsh) \quad (4)$$

Hydrocarbons are not usually present in components with high resistivity record values as shown by the 90-meter-thick tight limestone of the Avanah Formation (except for the porous zone). As a result, the upper part of the formation (AD) has a porosity of just 7%, which is low compared to the lower part of the formation, that is 80 meters thick and consists of dolomite, where the average porosity is 19%. This area has excellent fluid content and is known as Avanah Porous (AP).

Microscopically, different pore types were recognized in studied thin sections of the Avanah Formation in the Gomaspan outcrop according to Choquette and Pray (1970). The most common pore types are vuggy porosity which is formed as a result of the enlargement of fabric-selective pores including moldic and intercrystalline pores (Figure 3a). They are frequently present within dolomitic limestone beds in the lower part. Intracrystalline porosity also occurs within the lower part of the Avanah Formation in the Gomaspan outcrop (Figure 3a). Moldic porosity is common in the lower and middle part of the Gomaspan section and they are formed by the selective dissolution of various types of carbonate depositional grains (Flügel, 2010) (Figures 2a and c). Intraparticle porosity is also shown in the middle part of the carbonate rocks of the Avanah Formation, particularly within the benthonic foraminifera test (Figure 2a). Fracture porosity which are observed in the lower and upper part of the studied outcrop are mainly filled with a different type of cement (Figures 3a and c). Stylolitic porosity was also observed in the upper part of the formation and mainly filled by iron oxide cement (Figure 3c).

4.2.5 Water Saturation Model

The Indonesia model was used using Interactive Petrophysics software (version 4.4) to determine water saturation since the formation consists of shale and carbonate rocks. The water saturation for the Indonesia model was calculated using Equation 5 of Worthington's (1985) method.

$$[[Sw]]^{(n/2)}=\sqrt{(1/Rt)}/([[Vcl]]^{((1-Vcl/2))}/\sqrt{Rcl}+\sqrt{([[\varphi e]]^{m})}/\sqrt{(a*Rw)}) \quad (5)$$

where: Sw = water saturation (v/v); Vcl = clay volume (v/v); Rcl = clay resistivity (ohm.m); øe = effective porosity (v/v); Rw = formation water resistivity (ohm.m); Rt = true formation resistivity (ohm.m); m = cementation exponent (dimensionless); a = tortuosity (dimensionless) and n = saturation exponent (dimensionless).

Other petrophysical parameters were determined using the formula (Asquith and Gibson, 1982) in equations 6-12.

Hydrocarbon saturation (Sh) was determined by

$$Sh = 1- Sw \quad (6)$$

Water saturation of flushed zone (Sox) was

$$Sxo = Sw\ 0.2 \quad (7)$$

Residual hydrocarbon saturation (Shr) was determined by

$$Shr = 1- Sxo \quad (8)$$

Moveable oil saturation (MOS) was calculated from

$$MOS = Sxo – Sw \quad (9)$$

Moveable hydrocarbon Index (MHI) was calculated from

$$MHI =Sw/Sxo \quad (10)$$

Bulk volume water (BVW) was computed using

$$BVW= Sw*\varphi \quad (11)$$

Irreducible water saturation (Swirr) was evaluated using

$$Swirr = \sqrt{(F/2000)} \quad (12)$$

Saturation of the formation in the selected well has been shown in CPI for both units (Figures 9 and 10).

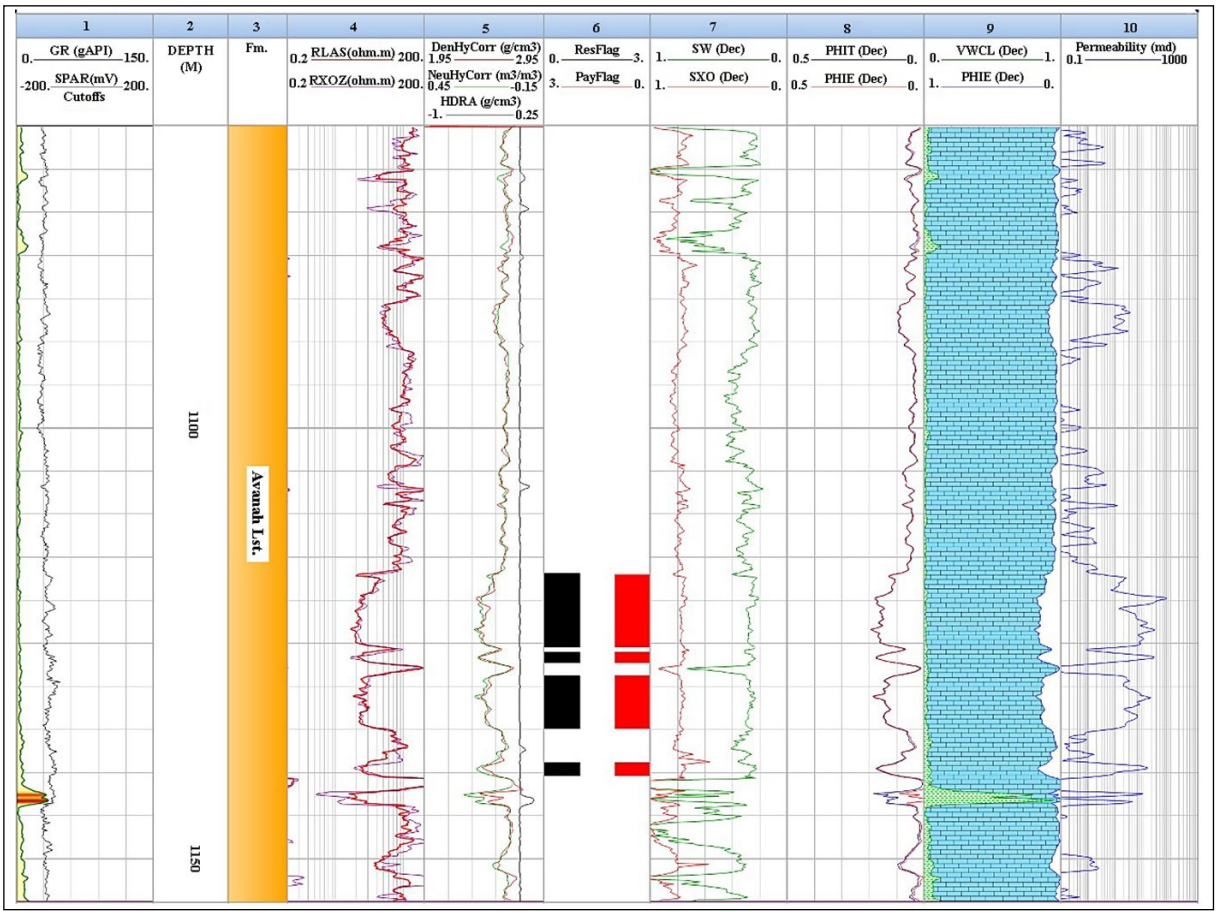

Figure 9- Computer processing interpretation for the dense part (limestone) of the Avanah Formation.

4.2.6.Relative Permeability (Kr) and Water Cut (WC)

The volume and kind of fluid produced, as well as the amount of water cut (WC), are the major considerations of any log analyzer. The relative permeability to oil and water (Kro and Krw, respectively) must be investigated. As earlier mentioned, the irreducible water saturation (Swirr) is used to examine these indications. Schlumberger (1986) generated several charts to demonstrate the relationship between Swirr and Sw. The next sector shows how such technology was used to the Avanah reservoir in the XX0 well. Figure (11) depicts the relative water permeability (Krw) of each component. The displayed locations that are composed of dolomite have a relative water permeability of less than 0.01. In addition, practically all sites are mapped on zero Krw (Figure 11a). The very low relative permeability to water implies the presence of a free water-producing reservoir (i.e., in an irreducible state), while the dens section has a large value of Krw (Figure 11b). Figure (12) displays the various relative permeability to oil (Kro) lines using a plot of Swirr versus Sw. The plotted points in this figure are clustered around only one (Kro = 100%) line. This demonstrates expected that the reservoir in the Khurmala oilfield would only produce oil. The cross-plot of the water cut (WC) for the study reservoir (Figure 13) reveals that the plotted points are grouped between 0 and 20% WC. This signifies that this reservoir has zones that will solely generate oil (less than 20 percent). The formation in the other part (which is composed of limestone) has sufficient relative water permeability values that range from 0.01 to 1. This means that the formation is oil-wet, and some water in the porous will move with oil during production. This conclusion has been reached by plotting Swirr versus SW to show watercut in this portion. It is evident that this parameter ranges from 20% to 60%.

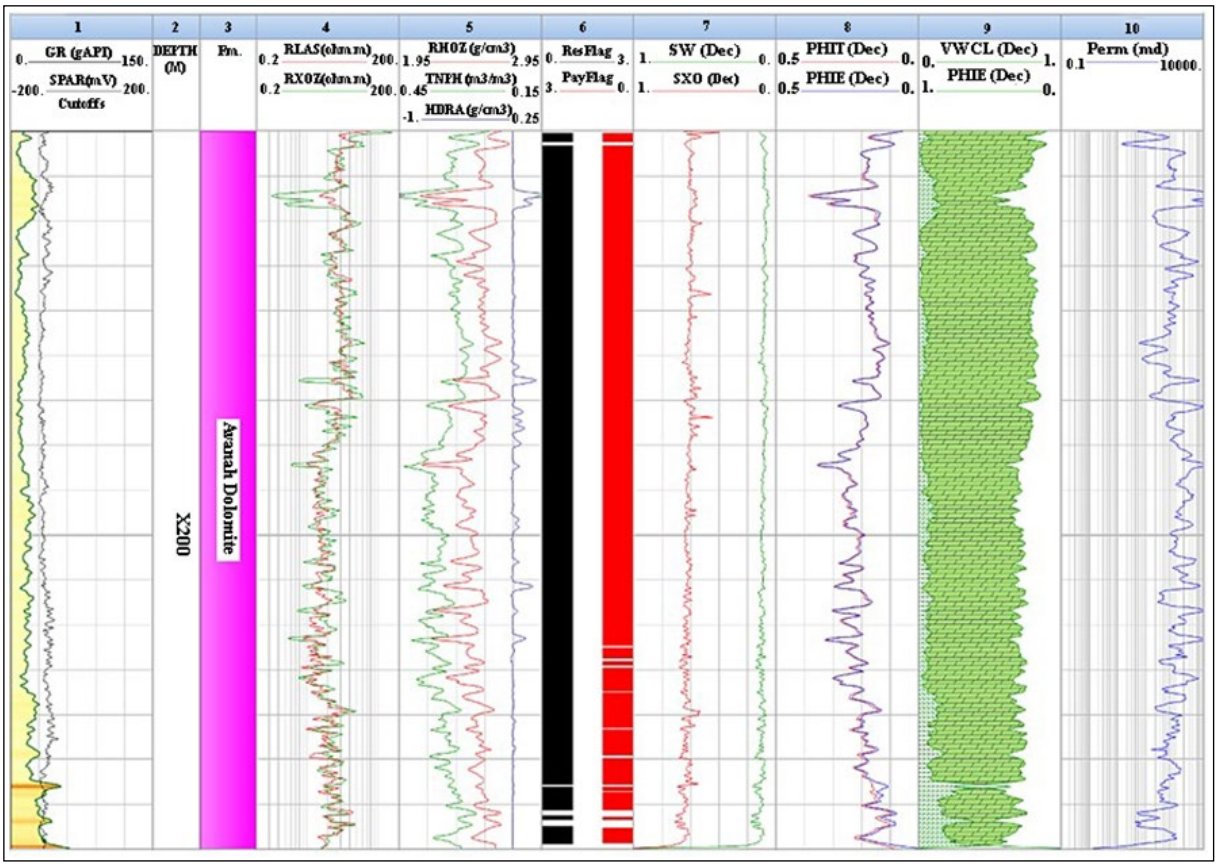

Figure 10- Computer processing interpretation for the porous part (dolomite) of the Avanah Formation.

4.2.7. Lithology and Mineralogy Model

The density-dependent cross-plot of neutron porosity for the selected well as shown in Figures (14 and 15), demonstrates that limestone and dolomite make up the bulk of the lithology of the Avanah Formation in the area under study. According to Schlumberger's (1998) assessment of the Rohmatrix vs. Umatrix cross plots, the shallower part of the formation is largely calcite, whereas the deeper part is predominantly composed of dolomite (Figure 16).

5. Discussion

The middle Eocene Avanah Formation in the Kirkuk oilfield which includes three domes; Avanah, Baba, and Khurmala domes was divided into two parts by the Iraqi Northern Oil Company (INOC) these are; the lower Avanah, the porous unit that is mainly composed of dolomite and dolomitic limestone and upper Avanah, the dense unit and is constituted mainly of limestone (Al-Hamdany and Sulaiman, 2014). Moreover, Musheer (2021) conducted petrophysical evaluations of the Avanah Formation in six wells of the Khurmala oilfield using TECHLOG software and concluded that the middle and northwest parts of the oilfield have good reservoir characteristics due to increasing porosity and permeability in addition to less of water saturation as compared to southeast part.

In the current study, the density-dependent cross plot of neutron porosity shows that the main lithology in the lower part of the Avanah Formation is dolomite while in the upper part is mainly limestone. This is also revealed from the Gomaspan outcrop section where dolomitic limestone is dominant in the lower and middle parts while the upper part is dominated by limestone. The clay concentration of the formation in the studied well as calculated by shale volume is 8% in part of dolomite (Avanah porous) and 4% in the upper limestone part (Avanah dense). The few contents of the clay which is less than 10% in whole Avanah Formation increase the effective porosity and permeability of the formation (Moradi et al., 2016).

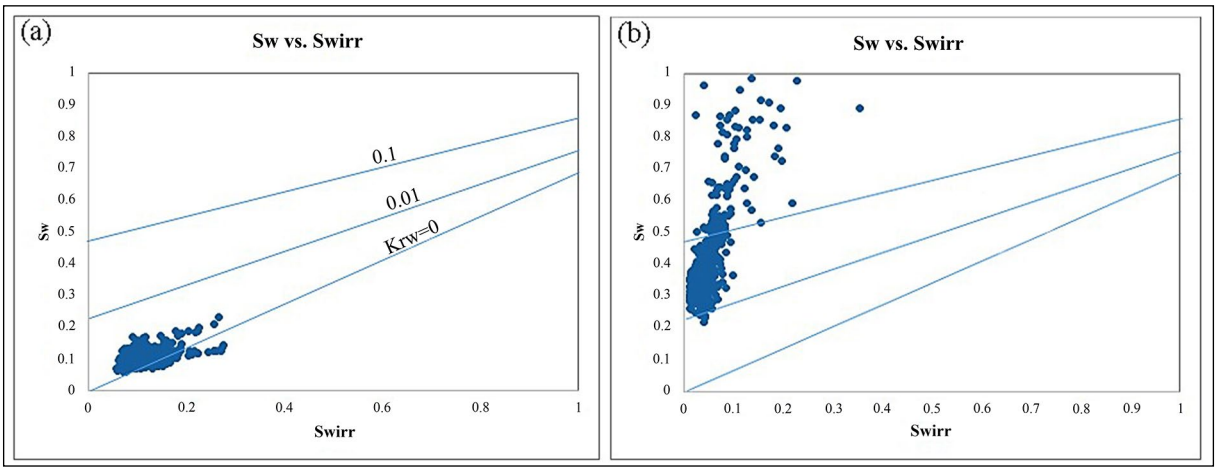

Figure 11- Cross plot between Sw versus Swirr for relative permeability to water (Krw) shows : a) Relative permeability of water related to Avanah dolomite. b) Relative permeability of water for Avanah limestone.

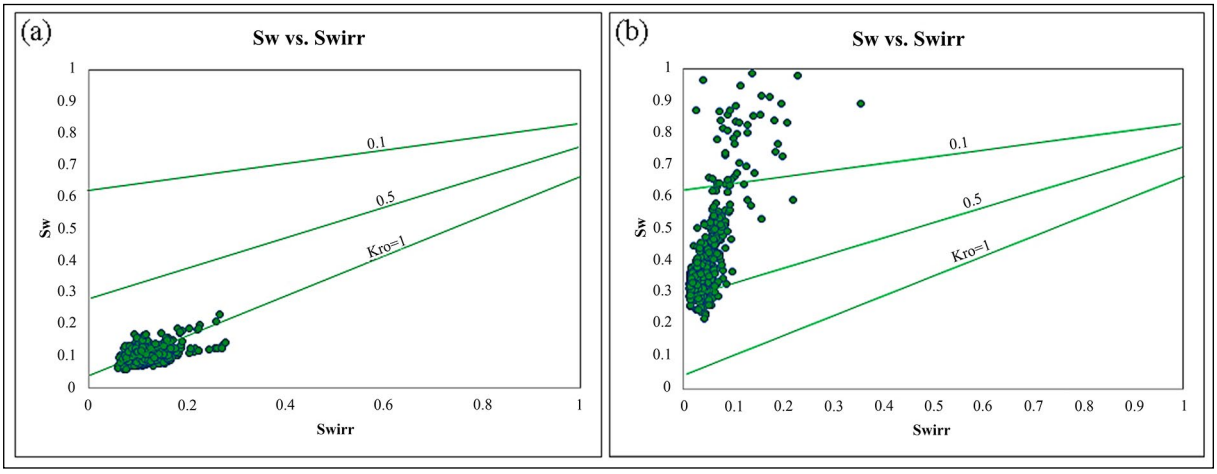

Figure 12- Cross plot between Sw versus Swirr for relative permeability to oil (Kro) shows: a) Relative permeability of oil related to Avanah dolomite. b) Relative permeability of oil for Avanah limestone.

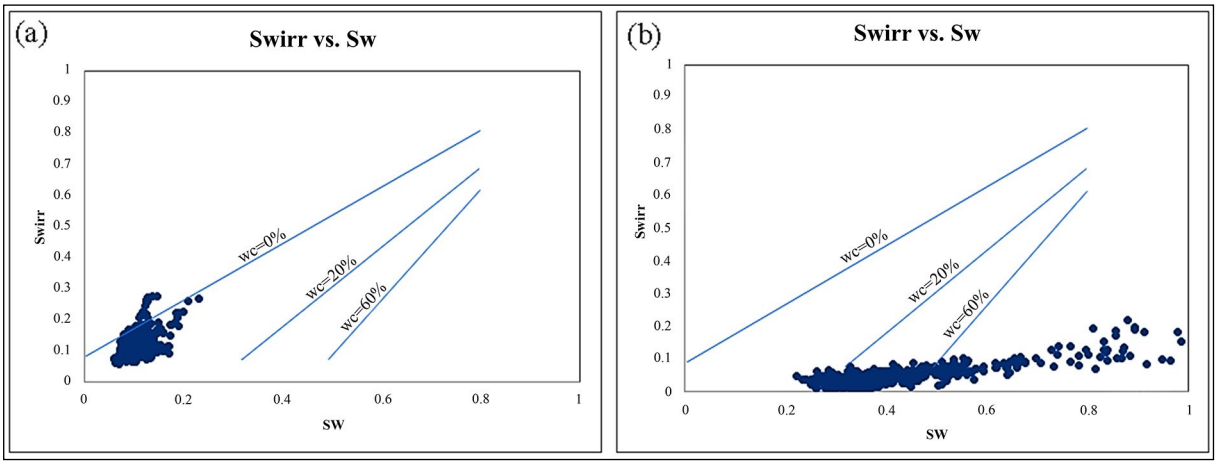

Figure 13-Cross plot between Sw and Swirr for the Avanah Formation, illustrating water cut percent: a) for Avanah dolomite, b) for Avanah limestone.

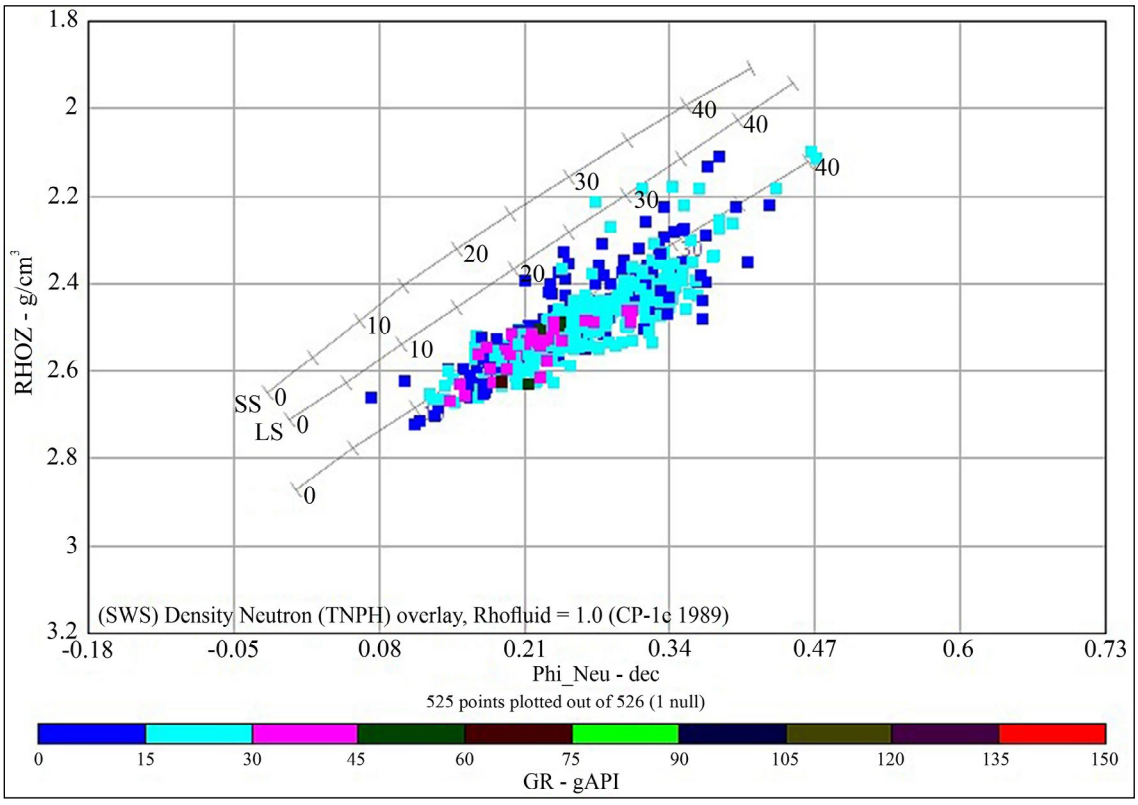

Figure 14- RHOB vs (NPHI) for lithology and porosity identification (Avanah porous).

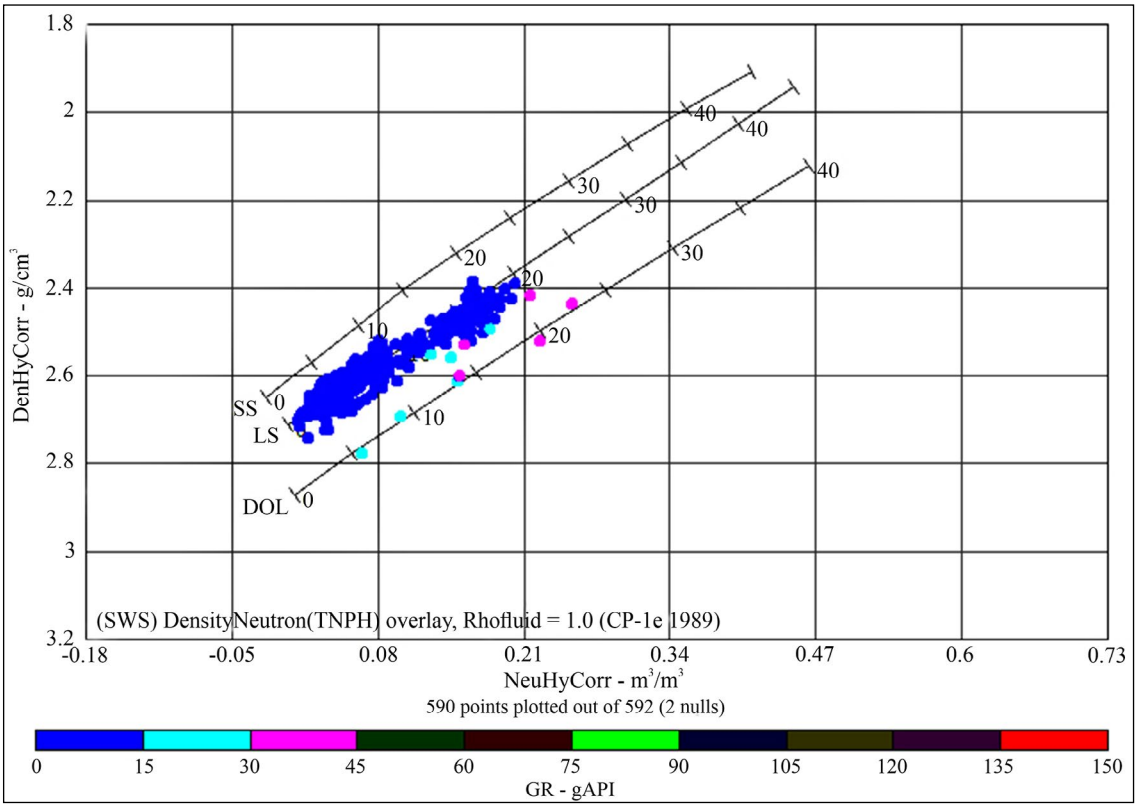

Figure 15- RHOB vs (NPHI) for lithology and porosity identification (Avanah dense).

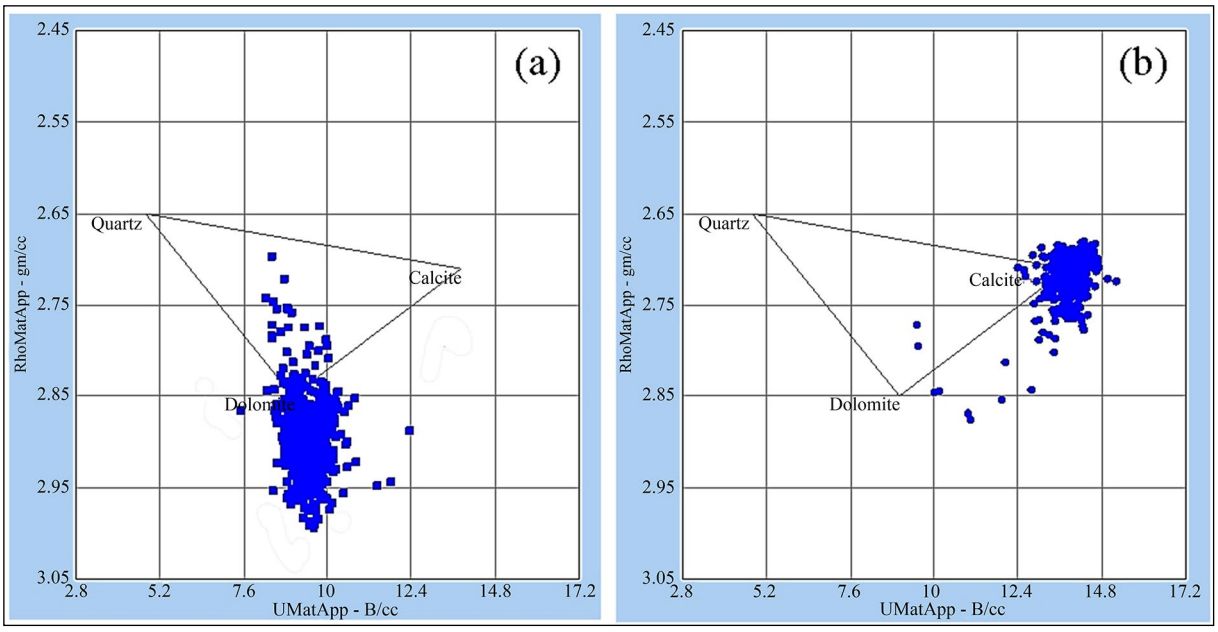

Figure16- Illustrates mineral identification of the Avanah Formation, dolomite (a) and calcite (b).

The lower dolomite part showed very low water saturation as revealed by equally dispersed points plotted around the hyperbolic line 0.02. Whereas, the upper limestone part contains more water as shown by random distributions along the hyperbolic line. The petrographic inspection of the Avanah Formation in the Gomaspan section confirms that the lower and middle dolomitic limestone part have secondary porosity mainly vuggy porosity formed from enlargement of intercrystalline dolomite pores by dissolution and moldic porosity formed

by dissolution of skeletal grains and they regarded as a major host of the hydrocarbon in the formation. Whilst, the upper limestone despite containing fracture and moldic porosity but most of them filled with calcite and iron oxide cement which decreases the permeability and leads to weakening the reservoir properties of the Avanah dense part.

The formation in the subsurface section contains no produced water and in the porous media have best movable hydrocarbon are present based on relative permeability for both oil and water, in addition, the formation has low water cut especially in the dolomite units which close to zero and in this part, a commercial hydrocarbon can be produced.

6. Conclusions

The Avanah Formation in the Khurmala oilfield, Erbil Governorate, Northern Iraq, is separated into two parts based on the formation's lithology; limestone and dolomite. A comprehensive investigation of the reservoir characteristics based on well-log data integrated with thin section investigations of the formation at Gomaspan outcrop revealed that the dolomitic part of the formation had a substantially larger void content than the limestone part. The main pore types are secondary porosity involves vuggy, moldic, intercrystalline, and fracture porosities mainly in the limestone part, and are filled with calcite and iron oxide cement. The fractures in the lower part of the Avanah succession in the Khurmala oilfield, include very low water saturation, implying substantial hydrocarbon saturation based on the relative permeability for oil and water, which is around 100 percent for the former and near zero for the latter. However, these findings are not inconclusive for the limestone fraction since it contains some hydrocarbons, especially in the lower part of the succession.

Acknowledgment

The authors express their deepest appreciation to the staff of NOC Company for providing our data for this research.

References

Al-Hamdany, A. M., Sulaiman M. A. 2014. Porosity of Avanah Formation and its Stratigraphical Distribution in Selected Wells of Kirkuk Oil Field. Iraqi National Journal of Earth Sciences 14(1), 49-66.

Asaad, I. S. 2022. Lithostratigraphy and microfacies analysis of Avanah Formation (Middle Eocene) in Gomaspan section northeast Erbil City, Iraq. Kuwait Journal of Science 49(3), 1-21.

Asaad, I. S., Omer, M. F., Ahmed, A. M. 2022*a*. Porosity Evolution and Microfacies Analysis of Khurmala Formation (Paleocene-Early Eocene) from selected sections in northern Iraq revealed by cathodoluminescence spectroscopy. Iraqi Geological Journal 55 (2F), 79-98.

Asaad, I. S., Al-Juboury, A. I., Bal Akkoca, D., Jha, P. 2022*b*. Petrography and mineralogy of rinded ferrous-carbonate concretions in the Middle Eocene carbonate rocks: A case study from the Avanah Formation in north-east Erbil City, northern Iraq. Geological Journal 57(8), 3021–3032.

Asquith, G., Gibson, C. 1982. Basic Well Log Analysis for Geologists. The American Association of Petroleum Geologist, 216.

Asquith, G., Krygowski, D. 2004. Basic Well Log Analysis. The American Association of Petroleum Geologist 244.

Awdal, A. H., Braathen, A., Wennberg, O. P., Sherwani, G. H. 2013. The characteristics of fracture networks in the Shiranish formation of the Bina Bawi Anticline; comparison with the Taq Taq field, Zagros, NE Iraq. Petroleum Geoscience 19(2), 139–155.

Balaky, S. M., Al-Dabagh, M. M., Asaad, I. S., Tamar-Agha, M., Ali, M. S., Radwan, A. E. 2023. Sedimentological and petrophysical heterogeneities controls on reservoir characterization of the Upper Triassic shallow marine carbonate Kurra Chine Formation, Northern Iraq: Integration of outcrop and subsurface data. Marine and Petroleum Geology 149, 106085.

Blunt, M. J., Bijeljic, B., Dong, H., Gharbi, O., Iglauer, S., Mostaghimi, P., Paluszny, A., Pentland, C. 2012. Pore-scale imaging and modelling. Advances in Water Resources 51, 197-216.

Buday, T. 1980. The Regional Geology of Iraq, Vol 1: Stratigraphy and Paleogeography. Geological Survey of Iraq, 445.

Catuneanu, O. 2006. Principles of sequence stratigraphy. Department of Earth and Atmospheric Sciences, University of Alberta, Canada. First Edition Elsevier Science Publishers Company Inc.

Choquette, P. W., Pray, L. C. 1970. Geologic nomenclature and classification of porosity in sedimentary 600 carbonates. AAPG Bulletin 54, 207 – 250.

Crain, E. R. 1986. The log Analysis Handbook. Penn-Well Publishing Company, Tulsa, Oklahoma, USA, 684,

Flügel, E. 2010. Microfacies of carbonate rocks, analysis, interpretation and application. Berlin: Springer-Verlag, 976.

Fouad, S. F. 2012. Tectonic Map of Iraq, Scale 1: 1000 000. 3rd edit, GEOSURV, Baghdad.

Friedman, G. M. 1959. Identification of carbonate minerals by staining methods. Journal of Sedimentary Research 29(2), 87– 97.

Gomes, J. S., Ribeiro, M. T., Strohmenger, C. J., Negahban, S., Kalam, M. Z. 2008. Carbonate reservoir rock typing e the link between geology and SCAL. In: Abu Dhabi International Petroleum Exhibition and Conference, 3-6 November 2008. SPE, Abu Dhabi, UAE, 14.

Gonfalini, M. 2005. The fundamental role of formation evaluation in the E and P process. STYPED "Sponsor Team for young petroleum Engineers Development.

Hamon, G. 2003. Two-phase flow rock-typing: another perspective. In: SPE Annual Technical Conference and Exhibition, 05 October 2003, Denver, Colorado, 12.

Moradi, S., Moeini, M., Al-Askari, M. K. G., Mahvelati, E. H. 2016. Determination of shale volume and distribution patterns and effective porosity from well log data based on cross-plot approach for a shaly carbonate gas reservoir. In IOP Conference Series: Earth and Environmental Science 44 (4), 042002.

Mukherjee S., Kumar N. 2018. A first-order model for temperature rise for uniform and differential compression of sediments in basins. International Journal of Earth Sciences 107, 2999– 3004.

Musheer, S. H. 2021. Petrophysical Assessment of Avanah Reservoir in Khurmala Dome of the Kirkuk Field, Iraq. MSc. Thesis, Near East University, Nicosia, Cyprus.

Neilson, J. E., Oxtoby, N.H. 2008. The relationship between petroleum, exotic cements and reservoir quality in carbonates e a review. Marine and Petroleum Geology 25 (8), 778-790.

Nnaemeka, E. 2010. Petroleum Reservoir Engineering Practice. Prentice Hall. United States, 700.

Pickett, G. R. 1972. Practical formation evaluation. G.R Pickett Inc, Golden. Colorado, 1445.

Schlumberger, 1986. Log Interpretation Manual/charts. Schlumberger, Housten, 125.

Schlumberger, 1998. Cased hole log interpretation principles/applications. Schlumberger Wireline and Testing, Houston, p. 198.

Sibley, D. F., Gregg, J. M. 1987. Classification of dolomite rock textures, Journals of Sedimentary Petrology 57, 967 – 975.

Tiab, D., Donaldson, E. C. 2004. Petrophysics, theory and practice of measuring rock properties and fluid transport properties, 2nd edn. Gulf Professional Publishing, Houston, 920.

Wanles, H. R. 1979. Limestone response to stress: Pressure solution and dolomitization. Journal of Sedimentary Research 49(2), 437 – 462.

Worthington, P. F. 1985. The Evolution of Shaly-Sand concepts in Reservoir Evaluation, The Log Analyst, 23-40.

Yang, Sh. 2017. “Fundamentals of petrophysics,” Petroleum Industry Press and Springer Verlag, Springe Geophysics. Germany, 502.